

Probing Length Generalization in Mamba via Image Reconstruction

Jan Rathjens¹[0000-0002-0490-538X], Robin Schiewer²[0000-0002-4021-2476],
Laurenz Wiskott¹[0000-0001-6237-740X], and Anand
Subramoney³[0000-0002-7333-9860]

¹ Institute for Neural Computation, Faculty of Computer Science,
Ruhr University Bochum, Bochum, Germany
`jan.rathjens@rub.de`, `laurenz.wiskott@rub.de`
² CITEC, Bielefeld University, Bielefeld, Germany
`robin.schiewer@uni-bielefeld.de`
³ Department of Computer Science,
Royal Holloway, University of London, Egham, UK
`anand.subramoney@rhul.ac.uk`

Abstract. Mamba has attracted widespread interest as a general-purpose sequence model due to its low computational complexity and competitive performance relative to transformers. However, its performance can degrade when inference sequence lengths exceed those seen during training. We study this phenomenon using a controlled vision task in which Mamba reconstructs images from sequences of image patches. By analyzing reconstructions at different stages of sequence processing, we reveal that Mamba qualitatively adapts its behavior to the distribution of sequence lengths encountered during training, resulting in strategies that fail to generalize beyond this range. To support our analysis, we introduce a length-adaptive variant of Mamba that improves performance across training sequence lengths. Our results provide an intuitive perspective on length generalization in Mamba and suggest directions for improving the architecture.

Keywords: Mamba · Length generalization

1 Introduction

Mamba [6] is a general-purpose sequence model within the class of state space models (SSMs). Compared to the ubiquitous sequence model transformer [12], Mamba offers reduced computational complexity while maintaining competitive performance across a broad range of benchmarks. The model has therefore seen widespread interest and adoption, particularly in natural language processing (NLP) [4, 6] but also in other domains such as vision [9, 15].

A central property of sequence models in general is length generalization, i.e., the ability of a model trained on sequences up to a certain length to maintain performance when evaluated on longer sequences. While the original work

on Mamba reported promising length generalization capabilities [6], subsequent studies [1–3, 10, 11, 14] have shown that Mamba often fails to generalize to longer sequences across a wide range of NLP tasks.

In this work, we investigate Mamba’s length generalization capabilities in a controlled vision-domain setting. Specifically, we train Mamba models to reconstruct Omniglot [8] characters from sequences of image patches of varying lengths. By generating reconstructions at different stages of sequence processing, we obtain indirect but interpretable evidence about the architecture’s processing mechanisms. Our setup enables targeted probing experiments to analyze these mechanisms systematically. We further compare Mamba’s performance with that of an analogous transformer baseline.

2 Related Work

Related work on length generalization in Mamba typically follows a common pattern: Studies report substantial limitations on an NLP task, identify architectural properties that may restrict length generalization, and propose targeted modifications. These modifications are then shown empirically to improve length generalization.

For instance, DeciMamba [2] and LongMamba [14] argue that Mamba learns an effective receptive field implicitly bounded by training sequence lengths. To mitigate this limitation, DeciMamba discards tokens deemed uninformative based on the magnitude of Δ_t , Mamba’s input-dependent discretization parameter that modulates hidden-state evolution based on the values of sequence tokens. LongMamba similarly utilizes Δ_t but discards tokens only for channels that are believed to encode global sequence information.

Attributing length generalization failures to out-of-distribution (OOD) accumulation of Δ_t for long sequences, MambaExtend [1] downscales this value at each time step. Similarly, MambaModulation [10] scales the state transition matrices based on the hypothesis that OOD growth or decay of state norms causes degradation when evaluating on longer sequences.

Taking a broader perspective, Ruiz and Gu [11] argue that long sequences induce OOD hidden-state distributions because training explores only a limited subset of attainable states. To mitigate this mismatch, they initialize the hidden state during training with the final state of a preceding sequence, thereby exposing the model to a broader range of state configurations.

Lastly, focusing on Mamba-2 [4], Chen et al. [3] attribute failures in length generalization to an overparameterized hidden state that hinders learning an effective forgetting mechanism for earlier tokens. They further argue that training sequence length should be balanced with hidden-state size.

While prior work offers valuable analyses of Mamba’s length generalization failures, the diversity of proposed explanations suggests that the underlying causes remain unclear. To complement these efforts, we investigate length generalization in a controlled vision setting and probe Mamba’s internal dynamics through interpretable visualizations.

3 Method

To generate interpretable visualizations during sequence processing, we consider an image reconstruction/completion task on 128×128 grayscale images of Omniglot characters [8]. Their structured, sparse strokes are easier to interpret than those of natural images.

An overview of the processing pipeline is shown in Figure 1. From each image, we sample an arbitrary number of potentially overlapping 4×4 patches at random spatial locations. Each patch is flattened and linearly projected to a 14-dimensional embedding vector.

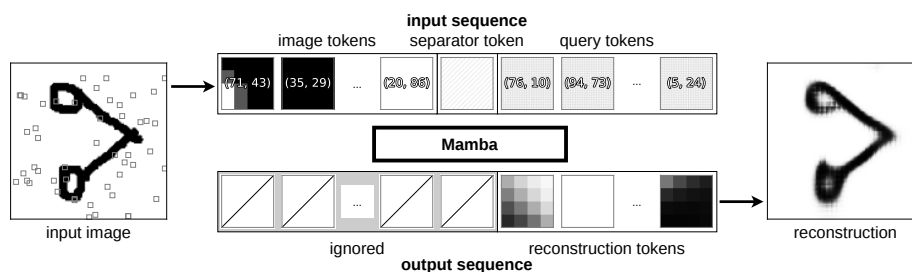


Fig. 1. Model overview. An input sequence of image patches augmented with spatial information, a separator token, and query tokens specifying spatial locations is processed by a Mamba model. The model produces reconstruction tokens, each predicting an image patch for the queried location. When query tokens densely cover the image, the reconstruction tokens can be assembled into a visualization of the input image.

To encode spatial information, we concatenate normalized (x, y) coordinates of the patch center to its embedding, yielding a 16-dimensional representation. We treat these representations as a sequence of tokens and refer to them as image tokens. We also evaluated an alternative positional encoding in which patches were embedded into 16-dimensional tokens and fixed sinusoidal encodings were added following standard transformer practice [12]. However, this configuration yielded slightly inferior performance compared to coordinate concatenation.

To the sequence of image tokens, we append a learnable 16-dimensional separator token that indicates the end of the image context. We then append a set of query tokens, each encoding a spatial location at which image information is requested. Specifically, a query token is obtained by applying a linear projection to the normalized (x, y) coordinates of the target location, resulting in a 16-dimensional representation. Target locations may coincide with sampled patches but may also lie at arbitrary positions within the image, in which case the model must interpolate the underlying image content.

We refer to the concatenation of image tokens, the separator token, and query tokens as the input sequence. This sequence is processed by a Mamba model, which produces an output token for each input token. The output tokens are

passed through a lightweight linear prediction head that preserves dimensionality. We discard outputs corresponding to image and separator tokens and retain only those corresponding to query tokens. These tokens represent predicted image patches at the queried locations and are referred to as reconstruction tokens. When query tokens densely cover the spatial extent of the image, the reconstruction tokens can be optionally assembled into a full image reconstruction for visual inspection. For the 128×128 images used in our experiments, 1024 query tokens suffice to cover the entire image. Beyond enabling visualization during processing, our setup also enables analyzing two distinct sequence-processing tasks: incorporating information from image tokens and responding to query tokens.

We train a standard Mamba architecture. Unless stated otherwise, our default configuration consists of eight Mamba blocks with model dimension 16 and state size 8, providing a favorable trade-off between reconstruction performance and computational cost. Our implementation builds on the Hugging Face Transformers library [13]. The only architectural modification is the removal of the depthwise convolution over the four most recent tokens at the beginning of each Mamba block. This operation is unnecessary in our setting because random patch sampling removes meaningful local ordering, increases computational overhead, and did not measurably affect performance.

Training is performed on the Omniglot training dataset with random rotation, translation, and scaling augmentations applied on the fly. For each batch, we sample a random number of image patches between 1 and a parameterized maximum T_I (default $T_I = 1024$). In addition, we use a fixed number of query tokens T_Q (default $T_Q = 1024$) to produce the output. Unlike image tokens, the number of query tokens can remain fixed because a reconstruction loss can be computed iteratively for each query token, which is not the case for image tokens.

The training objective minimizes the mean squared error (MSE) between reconstruction tokens and the ground-truth image patches at their query locations. Models are trained using standard deep learning techniques on NVIDIA A100 and H100 GPUs for approximately 16,000 epochs. Detailed hyperparameters and implementation specifics are provided in the accompanying code repository⁴.

4 Results

4.1 Quantifying Performance

We first evaluated the performance of trained Mamba variants on augmented Omniglot character images. Specifically, we tested models with different architectural settings, including the number of Mamba blocks, state dimensionality, and training sequence lengths T_I and T_Q (the number of image and query tokens during training). At evaluation time, we varied the number of image and query tokens provided to the model, denoted V_I and V_Q . Performance was measured as the MSE between the V_Q reconstruction tokens, queried at random spatial

⁴ <https://github.com/wiskott-lab/image-reconstruction-mamba>

locations, and their corresponding ground-truth patches, given V_I image tokens sampled from random locations.

Additionally, we compared our model against a transformer baseline configured under comparable conditions, i.e., identical token dimensions and varying T_I , T_Q , and model depth. The transformer encoder followed a Vision Transformer-style architecture [5], omitting the class token. A transformer decoder processed query tokens via cross-attention to the encoder’s image tokens (see the accompanying repository for implementation details).

Figure 2 summarizes the results. For Mamba (Left), the training image-token length T_I strongly influenced length generalization. Naturally, performance increased with increasing V_I as the models gained more knowledge of the input image. The best performances occurred when $V_I \approx 2T_I$. However, for larger values (e.g., $V_I \approx 4T_I$), reconstruction quality deteriorated sharply and quickly fell below chance. Interestingly, models trained with larger T_I values performed slightly worse on shorter sequences than those trained with smaller T_I .

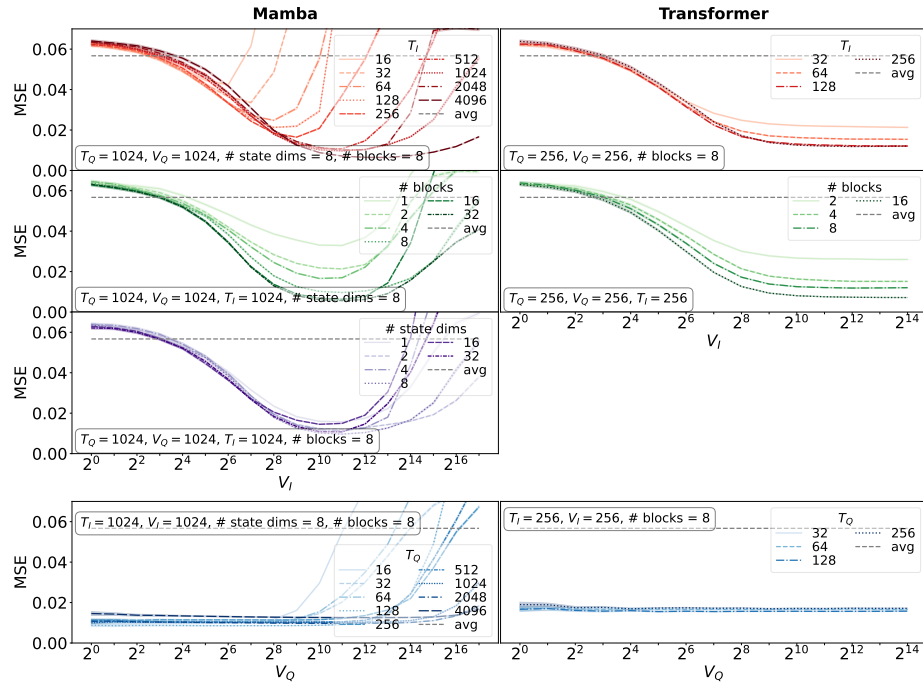


Fig. 2. Performance of Mamba (Left) and Transformers (Right) as a function of image and query token sequence lengths under different architectural settings. Curves show mean MSE on the Omniglot test set with 95% confidence intervals. Avg denotes a baseline that predicts the dataset-wide mean image patch.

Increasing model depth substantially improved overall performance but did not affect length generalization: performance consistently collapsed once V_I exceeded roughly $4T_I$. State dimensionality had a smaller impact. Small state sizes slightly degraded performance for $V_I \leq T_I$, but larger states did not consistently improve results or alter the generalization behavior. When varying T_Q (evaluated over V_Q in the bottom-left plot), performance again degraded once V_Q exceeded the training length. However, this effect occurred much later, around $V_Q \approx 16T_Q$, compared to the $4T_I$ threshold observed for image tokens. As with T_I , models trained with larger T_Q values performed slightly worse on short sequences, although the effect was less pronounced.

Transformer models exhibited different behavior. Due to the quadratic complexity of transformers, both training and evaluation were performed with shorter sequence lengths. As with Mamba, increasing T_I improved reconstruction quality. However, unlike Mamba, performance did not deteriorate when V_I substantially exceeded T_I . Instead, improvements saturated as V_I increased. Furthermore, the tendency of models trained with small T_I to perform slightly better on short sequences was much less pronounced than for Mamba. Increasing transformer depth improved reconstruction performance but did not affect length generalization. Similarly, varying T_Q showed no meaningful dependence on sequence length: Models achieved comparable performance across all V_Q values.

Several observations are noteworthy. Firstly, consistent with conflicting results in the literature, Mamba’s length generalization appears to be task-dependent: The model generalizes much better to increases in V_Q (querying information) than to increases in V_I (incorporating new image patches). We hypothesize that this difference occurs because query tokens do not introduce new information into the hidden state, making them easier to process.

Secondly, transformers exhibit strong length generalization despite frequently being reported to struggle with increasing sequence length in NLP tasks. We attribute this difference to our experimental setup, in which the model encounters all positional encodings during training. The strong generalization observed, therefore, supports prior work identifying positional encodings as a key bottleneck for transformer length generalization [7]

Thirdly, the number of state dimensions had no observable effect on length generalization. Hence, we were unable to reproduce the results of Chen et al. [3], who argued that an overparameterized state space causes failures in length generalization.

Finally, the performance curves of Mamba as a function of T_I closely resemble those reported by Ruiz and Gu [11] for Mamba-2 trained with different context lengths and evaluated on NLP tasks. This similarity suggests that our findings may extend beyond the image domain. Consistent with their observations, we identify the training context length (T_I or T_Q) as the primary factor influencing length generalization. For the remainder of our study, we focused on T_I , as our model is most sensitive to this parameter, and we expected reconstructions to remain reliable for query tokens within a reasonable range.

4.2 Probing Visualizations

Following the broad performance evaluation, we investigated the influence of T_I using the visualizations enabled by our setup. First, we provided models trained with different T_I values with varying numbers of identical image tokens and visualized the resulting reconstructions (Figure 3).

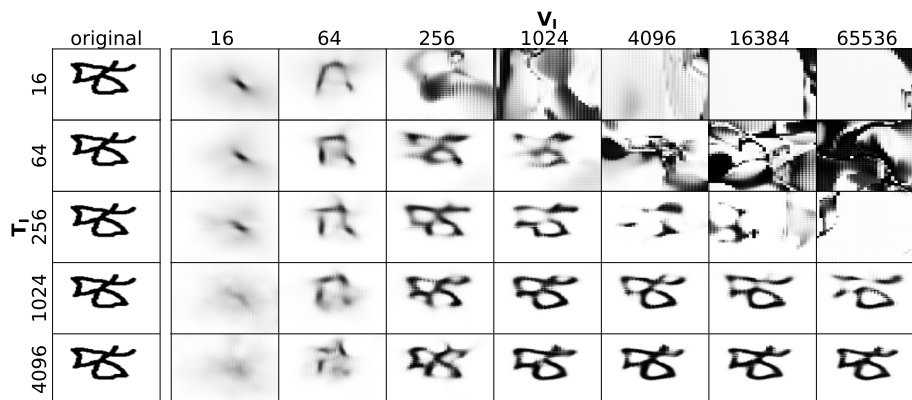


Fig. 3. Reconstructions across models. Column 1 shows the original image. Columns 2–8 show reconstructions given the indicated number of randomly sampled image tokens. Rows correspond to models trained with different T_I values.

Consistent with our performance evaluation, reconstruction quality improved as V_I increased. Beyond a certain point, however, each model exhibited a sharp degradation after which the original image was no longer recognizable. This breakdown occurred earlier for models trained with shorter context lengths. Interestingly, although identical image tokens were provided across visualizations, reconstructions sometimes differed systematically between models. For example, reconstructions in Column 2 show a higher-contrast center for models with smaller T_I , suggesting systematic differences in how the models process early observations.

To further investigate insinuated differences, we conducted two probing experiments. In the first experiment, we evaluated models on manipulated images in which the character appeared only in the top-left quadrant. We then processed random sets of image tokens from each quadrant using two scanning orders. In the first order, the top-left quadrant was processed first; in the second order, it was processed second (see Figure 4).

When the quadrant containing the character was processed first, both models reconstructed it accurately. However, for the model with $T_I = 1024$, the character gradually faded over time, whereas this effect was minimal for the model with $T_I = 4096$. Changing the scanning order significantly altered reconstructions:

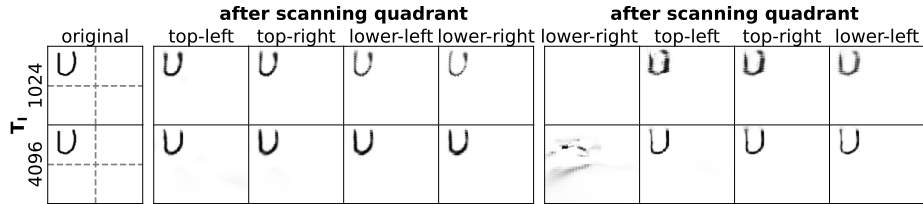


Fig. 4. Scanning an image in different orders. The left panel shows the original image. The middle and right panels display reconstructions of the image quadrants with different processing orders. Rows correspond to models with different T_I values.

The model with $T_I = 1024$ produced blurrier characters, whereas the model with $T_I = 4096$ produced weaker contrast.

In the second probing experiment, we examined how models respond to changes in the input image. Specifically, the model processed 16,384 tokens from one image, followed by 16,384 tokens from a second image, giving the model sufficient time to adapt to the second image. We generated reconstructions at intermediate steps (Figure 5 (Left)). Both models eventually adapted to the second image after observing sufficient tokens. However, the model trained with $T_I = 1024$ adapted much more rapidly: After processing 8192 tokens from the second image, its reconstruction reflected only the second image. In contrast, the model with $T_I = 4096$ still retained artifacts from the first image at the same point.

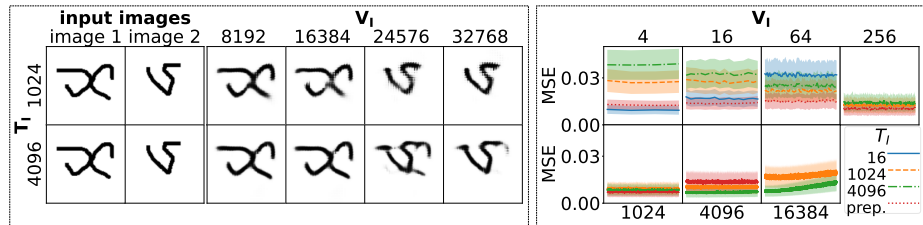


Fig. 5. (Left). Sequential processing of two images. Columns 1–2 show the original images. Columns 3–4 show reconstructions after processing tokens from the first image. Columns 5–6 show reconstructions after processing tokens from the first image, followed by those of the second image. Rows correspond to models trained with different T_I . **(Right).** Mean MSE of reconstruction tokens queried at spatial locations corresponding to the provided V_I tokens on the Omniglot test set (95% confidence intervals). Lines correspond to models trained with different T_I values and a sequence-length-adaptive variant (prepend Mamba).

Both probing experiments indicate qualitative differences in the models’ processing dynamics, particularly in how quickly they incorporate and update in-

formation over time. To support these qualitative observations with quantitative evidence, we measured how the MSE evolves during sequence processing for individual patches. Specifically, we queried only locations corresponding to image tokens whose spatial positions had already been observed and tracked how the reconstruction error at these locations changed over time. In this setting, the model already has full information about the queried patches, meaning that the MSE reflects only the model’s dynamics rather than additional information.

Both probing experiments illustrate qualitative differences in the models’ processing dynamics, particularly in how quickly they incorporate and update information over time. To quantify these observations, we measured how the MSE evolves during sequence processing for individual patches. Specifically, we queried only spatial locations corresponding to image tokens whose positions had already been observed. We tracked how the reconstruction error at these locations changed as additional tokens were processed. In this setting, the model already has full information about the queried patches, so the MSE reflects only the model’s internal dynamics rather than the availability of new information.

Results are shown in Figure 5 (Right) for models trained with three distinct T_I values and a modified Mamba variant called prepended Mamba, which we introduce in detail in the next section. The model trained with a small T_I value achieves low MSE for patches observed early in the sequence but fails to maintain this performance as additional tokens are processed. In contrast, models trained with larger T_I values initially exhibit higher MSE, but their performance improves as more tokens are processed, even for patches that have already been observed. This pattern suggests that although information from early image tokens is incorporated into the hidden state early in the sequence, it becomes accessible to query tokens only at later stages, unlike in models with small T_I , indicating a strong influence of T_I on the model’s processing speed.

The illustrated qualitative differences in processing observed for models trained with different T_I , supported by quantitative evidence, suggest that Mamba adapts its computational strategy to the sequence lengths encountered during training. Moreover, together with the performance evaluation in Section 4.1, which shows that models trained with small T_I perform better on short sequences than those with large T_I , our results indicate that Mamba implicitly learns to trade off performance across the sequence length regimes encountered during training.

4.3 Adapting Mamba

The observation that Mamba learns to trade off performance across sequence length regimes leads to several predictions. Firstly, restricting training to the upper half of the interval should improve performance within that range. To test this hypothesis, we trained a model with image token sequences lengths restricted to 512–1024 (referred to as truncated Mamba). Secondly, increasing the training interval should require sacrificing performance on short sequences to achieve better performance on longer ones. We tested this prediction by retraining our default model with $T_I = 65536$ (expanded Mamba). Finally, because Mamba

does not know the sequence length in advance, it cannot explicitly adapt its dynamics to varying sequence lengths and instead learns behavior that performs well on average across training lengths. To enable length-dependent adaptation of Mamba, we prepend a token encoding the sequence length to the input sequence (prepended Mamba), allowing the model to store this information in its hidden state and adjust its processing accordingly.

We report the performance of the adapted trained models in Figure 6 (Left), following the same evaluation protocol as in Section 4.1. As expected, truncated Mamba achieves slightly better performance within its training interval, though it degrades more sharply than the default model outside this range. As hypothesized, expanded Mamba sacrifices performance on short sequences while improving substantially on longer ones. The length-adaptive variant outperforms the default model across sequence lengths within T_I . This difference becomes particularly evident when querying only previously observed locations (see Figure 5 (right)), where prepended Mamba performs significantly better on short sequences than the default model with $T_I = 1024$. However, prepended Mamba also reduces length generalization compared to the default model.

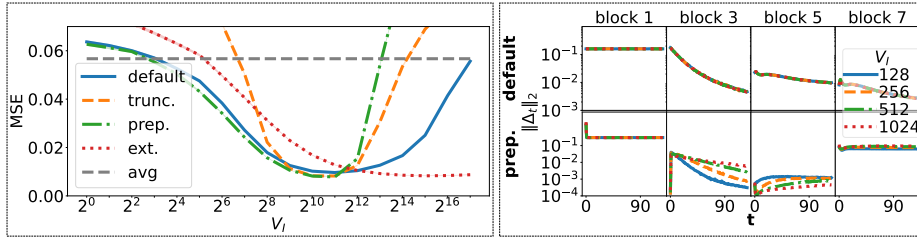


Fig. 6. (Left). Mean MSE of adapted Mamba variants across varying image-token sequence lengths, evaluated with 1024 query tokens on the Omniglot test set, with 95% confidence intervals. **(Right).** Each column corresponds to a representative block of the model. The top row shows the default model, and the bottom row shows the prepended Mamba variant. The curves depict the evolution of $\|\Delta_t\|_2$ over the first 128 tokens, indexed by t , for different V_I values, averaged across test sequences.

To verify that prepended Mamba indeed demonstrates length-adaptive behavior, we analyzed the evolution of the Euclidean norm $\|\Delta_t\|_2$ of the default model and prepended Mamba across blocks, averaged over test sequences of different lengths. Rather than interpreting absolute values, we examine whether the trajectory of $\|\Delta_t\|_2$ over image tokens varies with total sequence length, which would indicate adaptive hidden-state dynamics. Results for the first 128 tokens are shown in Figure 6 (right). For prepended Mamba, $\|\Delta_t\|_2$ evolves differently across sequence lengths, whereas in the default model it remains nearly invariant. Note that the average $\|\Delta_t\|_2$ for the first block is constant by design when tokens are drawn from the same distribution, since at this stage it depends only on the incoming token values and not on the hidden state. For prepended

Mamba, $\|\Delta_0\|_2$ differs because the first token is drawn from the distribution of sequence-length tokens rather than from the distribution of image tokens.

Our evaluation of the adapted Mamba variants provides additional evidence that Mamba trades off performance across the sequence lengths encountered during training: Training on longer sequences leads to significantly worse performance on shorter sequences, whereas restricting training to narrower length ranges or enabling sequence-length-adaptive behavior improves performance within the trained interval. However, the specializations also reduce length generalization.

5 Discussion

In this work, we set out to study length generalization in Mamba using a purposefully designed image reconstruction task that enables targeted probing of the model’s processing.

Our results suggest that Mamba does not learn a sequence-length-agnostic algorithm. Instead, it adapts its computational strategy to the sequence lengths encountered during training, particularly by adjusting processing speed. These adaptations lead to distinct behaviors across sequence-length regimes that do not transfer beyond the training distribution. In effect, the model optimizes a task-dependent trade-off across the sequence lengths observed during training. In contrast, transformers exhibit strong length generalization in our setting, likely because they are not required to extrapolate to unseen positional encodings.

The trade-off observed in our experiments raises the question of how related approaches (Section 2) achieve improved length generalization. The methods proposed in DeciMamba [2] and LongMamba [14] both rely on omitting tokens deemed unimportant during processing. Although these works demonstrate improved length generalization, Lu et al. [10] report that both methods perform worse than the default Mamba model on sequences of around 2000 tokens and outperform it only for longer sequences (≥ 4000 tokens). We expect this performance gap to be even larger for shorter sequences. In this sense, these methods are consistent with our findings, suggesting a trade-off across sequence-length regimes: Improvements on long sequences may come at the cost of degraded performance on shorter ones.

In contrast to DeciMamba and LongMamba, MambaExtend [1] and MambaModulation [10] report improved performance over the base model on both short and long sequences (although the evaluated sequences are not shorter than 2000 tokens). Importantly, their approaches differ from the former methods in that they introduce sequence-length-dependent scaling parameters. Therefore, their results are consistent with ours, which show that length-adaptive Mamba variants can alleviate the observed trade-off.

Sequence-length-adaptive mechanisms appear promising, but they also introduce an important limitation. Whether implemented by explicitly providing the sequence length at the beginning of the sequence, as in our approach, or through scaling mechanisms such as MambaExtend or MambaModulation, these meth-

ods require the sequence length to be known in advance. In many applications, however, the sequence length may not be known before processing begins. Nevertheless, our results also suggest that Mamba performs well across a range of sequence lengths, indicating that a rough estimate of the sequence length may already be sufficient.

Taken together, our results suggest that length generalization in Mamba is constrained by a trade-off in performance across sequence lengths. The model adapts to the sequence-length distribution encountered during training rather than learning a length-invariant algorithm. Understanding and controlling this trade-off may therefore be key to developing Mamba variants that maintain strong performance across a broader range of sequence lengths. In this context, sequence-length-adaptive mechanisms appear to be a particularly promising direction.

Acknowledgments. This work was partially supported by the RUB Research School through its PR.INT program.

Disclosure of Interests. The authors have no competing interests to declare that are relevant to the content of this article.

References

1. Azizi, S., Kundu, S., Sadeghi, M., Pedram, M.: MambaExtend: A Training-Free Approach to Improve Long Context Extension of Mamba. In: Proc. ICLR. pp. 97075–97090 (2025)
2. Ben-Kish, A., Zimerman, I., Abu-Hussein, S., Cohen, N., Globerson, A., Wolf, L., Giryes, R.: DeciMamba: Exploring the Length Extrapolation Potential of Mamba (2024), arXiv:2406.14528
3. Chen, Y., Zhang, X., Hu, S., Han, X., Liu, Z., Sun, M.: Stuffed Mamba: Oversized States Lead to the Inability to Forget (2024), arXiv:2410.07145
4. Dao, T., Gu, A.: Transformers are SSMS: Generalized Models and Efficient Algorithms Through Structured State Space Duality (2024), arXiv:2405.21060
5. Dosovitskiy, A., Beyer, L., Kolesnikov, A., Weissenborn, D., Zhai, X., Unterthiner, T., et al.: An Image is Worth 16x16 Words: Transformers for Image Recognition at Scale (2020), arXiv:2010.11929
6. Gu, A., Dao, T.: Mamba: Linear-Time Sequence Modeling with Selective State Spaces (2023), arXiv:2312.00752
7. Kazemnejad, A., Padhi, I., Ramamurthy, K.N., Das, P., Reddy, S.: The Impact of Positional Encoding on Length Generalization in Transformers (2023), arXiv:2305.19466
8. Lake, B.M., Salakhutdinov, R., Tenenbaum, J.B.: Human-level concept learning through probabilistic program induction. *Science* **350**(6266), 1332–1338 (2015). <https://doi.org/10.1126/science.aab3050>
9. Liu, Y., Tian, Y., Zhao, Y., Yu, H., Xie, L., Wang, Y., et al.: VMamba: Visual State Space Model (2024), arXiv:2401.10166
10. Lu, P., Huang, J., Zeng, Q., Wang, X., Wang, B., Langlais, P., Cui, Y.: Mamba Modulation: On the Length Generalization of Mamba (2025), arXiv:2509.19633

11. Ruiz, R.B., Gu, A.: Understanding and Improving Length Generalization in Recurrent Models (2025), arXiv:2507.02782
12. Vaswani, A., Shazeer, N., Parmar, N., Uszkoreit, J., Jones, L., Gomez, A.N., et al.: Attention Is All You Need (2017), arXiv:1706.03762
13. Wolf, T., Debut, L., Sanh, V., Chaumond, J., Delangue, C., Moi, A., et al.: HuggingFace’s Transformers: State-of-the-art Natural Language Processing (2019), arXiv:1910.03771
14. Ye, Z., Xia, K., Fu, Y., Dong, X., Hong, J., Yuan, X., et al.: LongMamba: Enhancing Mamba’s Long Context Capabilities via Training-Free Receptive Field Enlargement (2025), arXiv:2504.16053
15. Zhu, L., Liao, B., Zhang, Q., Wang, X., Liu, W., Wang, X.: Vision Mamba: Efficient Visual Representation Learning with Bidirectional State Space Model (2024), arXiv:2401.09417